Superconducting Bolometer Array Architectures

Dominic J. Benford[*1a], James A. Chervenak[a], Kent D. Irwin[b],
S. Harvey Moseley[a], Rick A. Shafer[a], Johannes G. Staguhn[a,c], Ed J. Wollack[a]

a NASA / Goddard Space Flight Center *b* NIST – Boulder *c* SSAI

ABSTRACT

The next generation of far-infrared and submillimeter instruments require large arrays of detectors containing thousands of elements. These arrays will necessarily be multiplexed, and superconducting bolometer arrays are the most promising present prospect for these detectors. We discuss our current research into superconducting bolometer array technologies, which has recently resulted in the first multiplexed detections of submillimeter light and the first multiplexed astronomical observations. Prototype arrays containing 512 pixels are in production using the Pop-Up Detector (PUD) architecture, which can be extended easily to 1000 pixel arrays. Planar arrays of close-packed bolometers are being developed for the GBT and for future space missions. For certain applications, such as a slewed far-infrared sky survey, feedhorn-coupling of a large sparsely-filled array of bolometers is desirable, and is being developed using photolithographic feedhorn arrays. Individual detectors have achieved a Noise Equivalent Power (NEP) of ~10^{-17} W/√Hz at 300mK, but several orders of magnitude improvement are required and can be reached with existing technology. The testing of such ultralow-background detectors will prove difficult, as this requires optical loading of below 1fW. Antenna-coupled bolometer designs have advantages for large format array designs at low powers due to their mode selectivity. We also present a design and preliminary results for an enhanced-dynamic–range transition edge sensor suitable for broadband ultralow-background detectors.

Keywords: superconducting bolometer array, transition edge sensor, superconducting multiplexer, SQUID multiplexer

1. INTRODUCTION

Recently, the National Academy of Sciences recommended some major long-term mission goals for the far-infrared to millimeter region[1]. One of these is SAFIR, the Single Aperture Far-Infrared Observatory, which is envisioned as a larger, colder NGST for the 20μm-800μm region[2,3]. Another is CMBPOL, a mission to measure the polarization in the microwave background radiation. A third, though less defined, is a submillimeter interferometer similar to the SPECS mission[4]. All these missions have several things in common, such as cryogenic optics and large collecting areas. Another similar requirement is on large, sensitive detector arrays.

The largest submillimeter detector array manufactured to date is the semiconducting bolometer array made for SHARC-II and its companion for HAWC[5]. This array contains 384 pixels, each of which has a noise equivalent power (NEP) of about 10^{-16} W/√Hz. Richard's Law states that the number of pixels in an array divided by the square of their sensitivity – the metric defined by the Bahcall report[6] – doubles every year[7]. The metric for the largest bolometer array to date is $4 \cdot 10^{34}$ pixels/W^2/s. The camera for SAFIR[8] will require a 128^2 array of bolometers with an NEP of 10^{-19} W/√Hz, for a value of $1.6 \cdot 10^{42}$ pixels/W^2/s. Spectroscopy from a cold telescope with a modest array (32^2) of $3 \cdot 10^{-21}$ W/√Hz detectors requires a value of ~10^{44} pixels/W^2/s. These values are about 9 orders of magnitude improved relative to today's detectors, which Richard's Law claims would take 30 years! However, Richard's Law is true only when averaged over long times; evolutionary developments are probably slower, while revolutionary developments may be much faster.

A recent development is the superconducting bolometer read out by a multiplexed SQUID amplifier[9]. Because of their high sensitivity and the existence of an efficient multiplexing technology, superconducting bolometer arrays are the most promising technology for meeting sensitivity and pixel count requirements of upcoming far-infrared to millimeter-

[1] Corresponding Author: Dominic J. Benford; dominic.benford@gsfc.nasa.gov; 301.286.8771; Code 685, NASA/GSFC, Greenbelt, MD 20771; http://lasp-nts1.gsfc.nasa.gov/irbranch/Dominic_J_Benford.html

Millimeter and Submillimeter Detectors for Astronomy, Thomas G. Phillips, Jonas Zmuidzinas, Editors, Proceedings of SPIE Vol. 4855 (2003) © 2003 SPIE · 0277-786X/03/$15.00

wavelength instruments. Some of the advantages include:

- Superconducting thermistors feature good noise performance, high sensitivity, high speed, linear behavior, and few strange effects
- Superconducting bolometers have much simpler thermal interfaces than semiconducting bolometers
- Multiplexed readouts have been developed, permitting large arrays with simple electronics
- Superconducting bolometer arrays benefit from thin film micromachining techniques, robust superconducting materials systems, and the extreme intrinsic sensitivity of superconducting thermometers
- Close-packed architectures are being developed to permit large format (>1000 elements) filled arrays with high efficiency

2. ASPECTS OF SUPERCONDUCTING BOLOMETER ARRAY FABRICATION

2.1 Superconducting transition edge sensors

The fundamental change in a superconducting bolometer is the replacement of the semiconducting thermistor with a superconducting thermistor, called a transition edge sensor (TES). The sensitivity of any thermistor can be expressed in terms of a unitless constant α, often referred to as the sensitivity:

$$\alpha \equiv \frac{d\log R}{d\log T} = \frac{T}{R}\frac{dR}{dT}.$$

For semiconducting thermistors, the hopping conduction model predicts:

$$R(T) = R_0 \exp\left(\sqrt{\frac{T_0}{T}}\right) \quad \therefore \quad \alpha = \frac{1}{2}\sqrt{\frac{T_0}{T}}$$

where T_0~30K and bias temperature of T~0.3K are achievable, yielding α≈15 for a sensitive thermistor. For a superconducting thermistor, there is no clear analytic function, so the simplest approximation is:

$$\alpha \equiv \frac{d\log R}{d\log T} = \frac{T}{R}\frac{dR}{dT} \approx \frac{2T_C}{\Delta T}$$ where ΔT is the approximate transition width.

With actual data on a TES, an approximate function can be fit to help derive the sensitivity[10], where the transition width is measured at the 10% and 90% levels of the *R(T)* curve:

$$R(T) \sim \frac{R_N}{2}\left[\tanh\left(\pi\alpha\left(T - T_C\right)\right) + 1\right] \quad \therefore \quad \alpha \approx \frac{T_C}{R_N}\left(\frac{0.8R_N}{T_{90\%} - T_{10\%}}\right).$$

It is not uncommon for the sensitivity of a superconducting thermistor to be 1000, as shown in Figure 1.

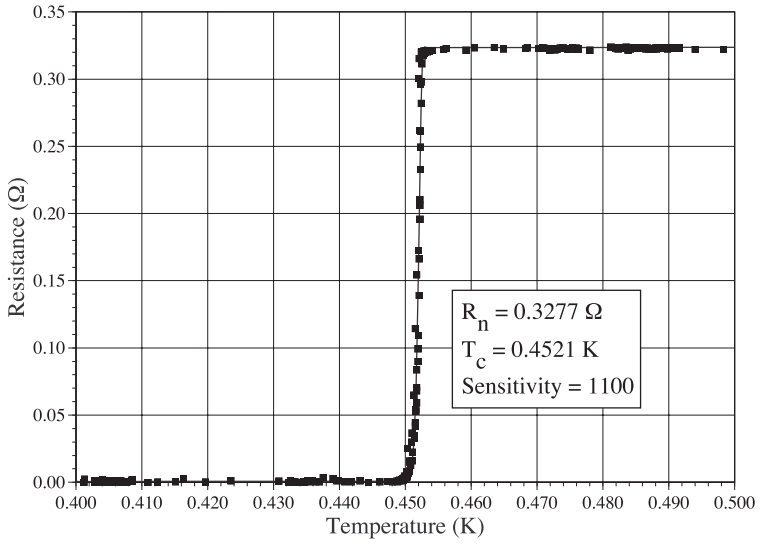

Figure 1. Resistance of a superconducting transition edge sensor as a function of temperature near the transition.

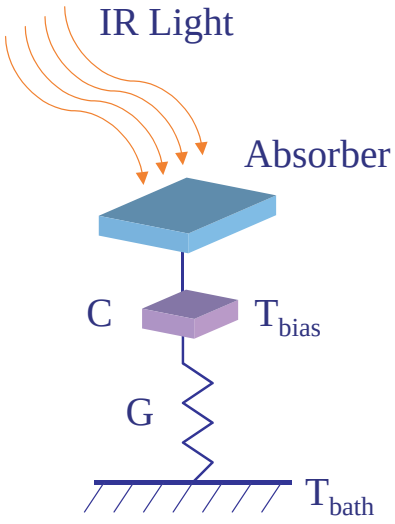

Figure 2. Simple thermal model of a bolometer.

According to a simple model for a TES bolometer (shown in Figure 2), the response time of a bolometer is typically the thermal time constant, $\tau = C/G$. However, TES bolometers can be faster by means of negative electrothermal feedback. When biased onto the transition, power is dissipated in the thermistor as $P = V^2/R$. When optical power is applied, the thermistor warms up, increasing its resistance dramatically. The bias power drops to compensate, bringing the TES back towards the stable bias point. The effective time constant is then approximately $\tau_{eff} = \tau n/\alpha$, where n is the temperature index of the thermal conductance. At low frequencies ($(\omega\tau_{eff})^2 \ll 1$), the Johnson noise is suppressed through the action of the electrothermal feedback by a factor of $(n/\alpha)^2$. The end result of this is that the intrinsic noise of a TES bolometer is typically dominated by the phonon noise alone.

A TES can be made in any superconducting material; the only requirements are that it feature a sharp transition of known and repeatable transition temperature and normal resistance. In order to realize these criteria, common approaches include superconducting/normal metal bilayers and trilayers and bulk superconductors (such as W) with magnetic dopants. The bilayer approach uses the proximity effect in the normal metal to suppress the superconductivity in the other metal; this permits the transition temperature and resistance to be modified by changing the thicknesses of the two layers. A photo of a Mo/Cu bilayer is shown at right in Figure 3.

Figure 3. Mo/Cu bilayer with contact pads (on ends) and normal metal bars along the sides to suppress edge effects.

2.2 Fabrication techniques for large format arrays of sensors

Array production requires a scaleable architecture into which robust components can be integrated reproducibly. Here we describe the materials and processing techniques that enable robust detector elements for large formats, including the superconducting bilayer, wiring, and thermal isolation.

The first issue is choosing a suitable bilayer system for a building block in a large format array and demonstrating that the chosen materials are capable of optimal noise performance. The collaboration between NASA's Goddard Space Flight Center and NIST-Boulder has extensive experience with two materials system, Mo/Au and Mo/Cu, for which we can identify different strengths depending upon the application. Numerous candidate materials systems are being pursued by the community and this discussion only points out strengths of our materials choice without ruling out these many other options.

Stability and Uniformity:

The two binary systems, Mo/Cu and Mo/Au, are similarly immiscible for long term device stability against elevated temperatures and aging. Each system is readily deposited with uniformity over a silicon wafer using either e-beam or magnetron sputter deposition and exhibit wafer-to-wafer reproducibility of electrical properties such as bilayer T_C and R_N. Both are good materials systems for array production, although certain features lend Mo/Cu some advantages for bolometer arrays. Au films need to be thicker to produce the same T_C, leading to lower impedance and higher heat capacity. The trend in these parameters is more suited to X-ray microcalorimeters than infrared bolometers. Higher device impedance relaxes multiplexer sampling constraints, potentially increasing the number of detectors read out.

Selective Etch:

For Mo/Au, a chemical etch that selectively etches gold without attacking the molybdenum has proved elusive. Since the Mo film tends to be thin, even in large heat capacity devices, etching the gold layer results in the Mo tending to get undercut and possibly corroded during wet processing. This undercut can affect device performance, since materials properties can be especially susceptible to this effect in the thin film limit, as in bolometers. While this is not a severe problem for small numbers of devices, it is a liability for large format arrays. In contrast, for the Mo/Cu process, there exist selective wet and dry etches between Mo and Cu that allow for flexibility during process flow.

Corrosion resistance:

The Au toplayer is robust to typical environmental conditions so that no corrosion proofing is necessary. Cu requires treatment with benzotriazole (a process introduced to TES fabrication by Gene Hilton of NIST-Boulder), but is

straightforward to protect devices from corrosion. This treatment is useful for protecting the device copper during processing as well as sealing devices from the environment after they have left the clean room.

Lead integration:
While a practical point rather than a fundamental one, integrated leads – wiring for the TES made from the same superconducting material – are good for large format arrays, as they reduce the number of interconnects in the array. Mo/Cu has a more straightforward route to producing integrated leads than Mo/Au: just selectively etch away the Cu and the Mo leads remain. Integrated Mo leads must be formed on Mo/Au detectors using physical etching such as ion milling, or by placing additional material on top of the Mo/Au layer. Both these processes should be developable for large formats.

Process flow:
Here we describe briefly the processing done for the Mo/Cu bolometers shown elsewhere in this paper. While this is not the only possible process flow, it is a valid complete example.

(1) Mo/Cu DC magnetron sputtered in high vacuum chamber
(2) Toplayer treated with 1% benzotriazole in DI, which forms an organometallic anticorrosive layer on copper films. This technique was adapted from a treatment originally applied to TES processing at NIST-Boulder.
(3) Cu etched to form device layer using ammonium persulfate etchant
(4) Mo etched to form device and leads – CF_4 based reactive ion etch (RIE) to prevent undercutting, as Mo etchants are aggressive to Cu.
(5) Liftoff resist for deposition of Cu bars/Al contact pads/on-chip shunt resistors and other features. In situ ion mill before deposition. (Bilayer process where top layer is acetone soluble to liftoff metal, bottom layer is removed by a different solvent to protect narrow wiring, device copper features while in liftoff)
(6) Backetch up to the buried etch stop using deep RIE, resulting in a freestanding membrane; followed by frontetch of membrane to produce micromachined suspended bolometer with tailored thermal conductance.
(7) Structures can be folded like Pop-Ups (SHARC II/HAWC) or bump-bonded onto fanout board (SCUBA II). Both types of arrays are under development.
(8) Absorber can be shadowmasked (Bi resistive sheet) or lithographically integrated (resistor grid)

2.3 Noise performance and optimization
The noise spectrum of a TES bolometer is a combination of noise from several sources. In the band of interest, the noise is typically dominated by phonon noise, which rolls off above the time constant. Johnson noise appears only above this frequency, as it is suppressed at low frequencies by electrothermal feedback. At very high frequencies (above the Nyquist frequency), the Johnson noise rolls off to the SQUID noise floor. This SQUID noise is assumed to be white, and by design is less than the other noise sources in the band of interest. At low frequencies, there is empirical 1/f noise, the origin of which is poorly understood. The combined noise spectrum is shown in Figure 4, where an approximate noise model is fit to a measured Al/Ag bilayer TES manufactured at NIST-Boulder. The model shows good agreement with the data, and very little spurious noise is evident. The noise spikes at 60Hz and its harmonics are visible, as is a slight excess noise at ~5Hz.

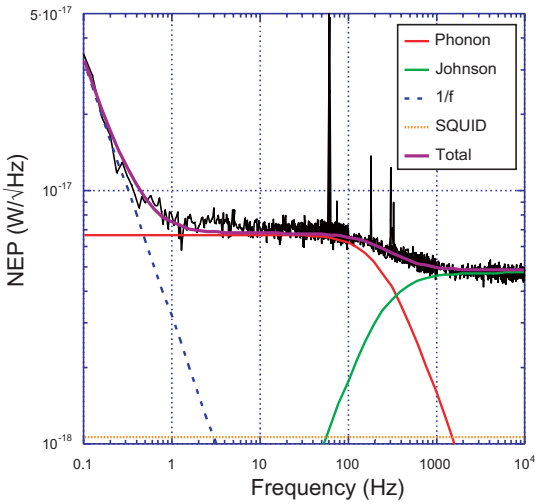

Figure 4. Measured vs. modeled noise of a TES bilayer.

One known source of excess noise is an additional thermal noise bump at frequencies of ~100Hz, several octaves wide. This is understood to arise from additional heat capacity thermally separated from the TES sensor element. This is a readily solved problem, by increasing heat capacity of the detector relative to the membrane and absorber structures. Knowing that this problem exists, we have been able to correct for it.

There are also noise sources known to be electrical effects related to the dynamics of the superconducting/normal metal region. An adequate description of this noise mechanism requires empirical exploration of geometric and other effects (e.g., boundary conditions of biased detector element, current density, internal heat capacity distribution to normal and superconducting regions). We have observed that placing normal metal bars along the edges of the bilayers greatly improves the performance of biased TES bolometers (Figure 5). At the time, the improvement was attributed to wet etch nonuniformities in the Au layer. However, recent measurements by other groups on X-ray calorimeters suggest that engineering the transition to control dynamic effects among the superconductor/normal interfaces in the biased sensor leads to better noise performance[11]. We have begun studying how edge conditions can also be used for transition engineering.

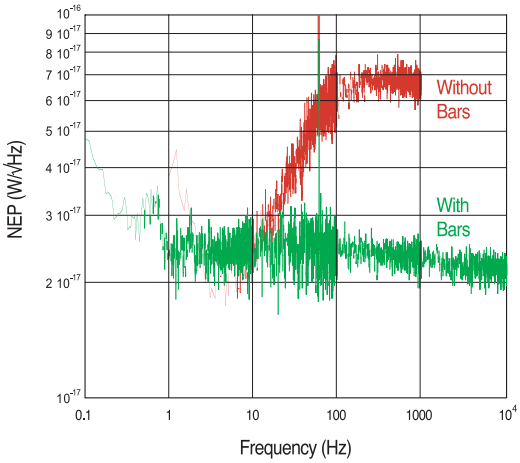

Figure 5. Noise in Mo/Au with no edge treatment versus a Mo/Cu layer with thick copper bars along the edges.

2.4 Transition engineering

Optimizing the behavior in the TES while biased onto the transition is an important but complex aspect of superconducting bolometers. As discussed above, controlling the normal metal boundary conditions at the edge of a rectangular TES has been shown to help the noise performance in lithographed sensors. A possible additional aspect of the transition is the separation of the normal and superconducting regions. It seems logical to avoid geometries and/or impedances that cause phase separation in the TES[12], while exploring possible ways to modify dynamics of superconductor biased in its transition. It has been reported[13] that a TES with normal regions transverse to the bias current can suppress mid-band noise in a microcalorimeter. To some extent, this technique introduces an artificial phase separation into the detector by intentionally driving regions of the detector normal so that no dynamics associated with the supercurrent can propagate through these regions. There is a large impedance difference between the typical TES microcalorimeter (10 mΩ) and the devices in which thermal transport induced phase separation has been observed (2-5 Ω). In our case, since infrared bolometers often have higher impedance (approaching the resistances at which phase separation occurs), it might not be possible to drive the film normal in this fashion.

On the following page, we show several TES bilayers with different normal metal bar geometries (Figure 6). The width of the transition changes as these shapes change. For instance, we can associate a sharper transition with narrower bars (i.e. bar width to detector width ratio is smaller). We have also implemented wedge-shaped and bowtie-shaped boundaries on similar devices, in an attempt to engineer the way normal/superconducting interfaces set up in the detector, making it more difficult for the interfaces to fluctuate and interact over large length scales.

2.5. SQUID Multiplexers

We have tested an 8-input SQUID multiplexer to verify properties relevant to far-infrared detector arrays: is the channel-to-channel crosstalk low, and does the SQUID multiplexer permit the readout of Johnson noise-limited sensors? The multiplexer was fabricated at NIST-Boulder as described by Chervenak at al. (1999)[14]. For our crosstalk measurements, one sine wave and one triangle wave input each were fed into a cold electronics setup so as to mimic the modulation of a signal from infrared light. The multiplexed amplifier was switched between these inputs, amplified, digitized, and demultiplexed to recover the original input waveforms (Figure 7). The performance features low distortion with $\ll$1% typical crosstalk, highlighting the excellent fidelity of the amplifier. It should be pointed out that the TES is biased at all times, and is low-pass filtered using an inductor with time constant $L/R \approx$ 20μs to a response time slower than the multiplex switching time. Effectively, the inductor and TES integrate the signal, so that the multiplexer samples an integrated signal; no loss of signal-to-noise is introduced even though the signal from each TES is read out for a shorter time. This is true provided that the noise contribution of the SQUID and room temperature electronics is substantially less (by a factor of more than $\sqrt{n}$) than that of the TES. Furthermore, in order to remain stable, the devices must be sampled faster than $f_{L/R}=(3+2\sqrt{2})\, f_{\mathrm{TES}} \sim$100kHz[15].

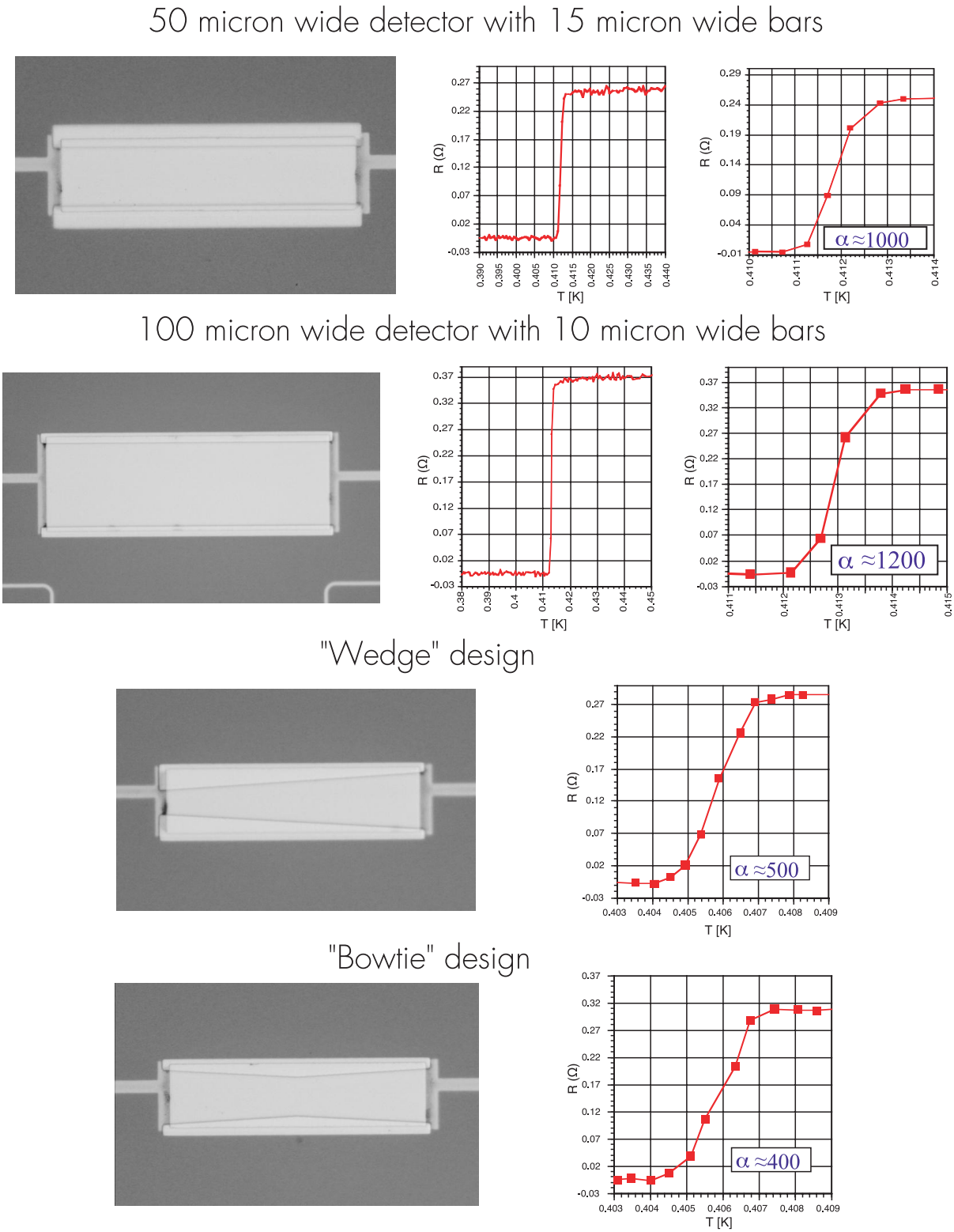

Figure 6. We show several geometries of boundary-condition normal metal bars applied to similar TES bilayers; to their right is the R(T) curve showing the change in sensitivity. All of these devices exhibit sharp enough transitions to enable strong electrothermal feedback, and so the most important difference between them will be their noise performance, which we have yet to measure.

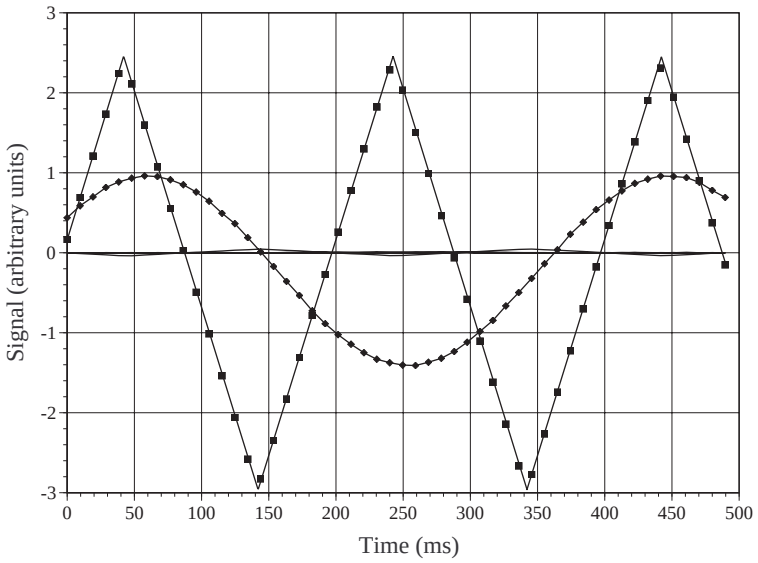

Figure 7. Time series of data from eight demultiplexed SQUID multiplexer channels. One SQUID channel has a sinusoidal input flux (diamonds), one has a triangle-wave input flux (squares), and the rest have no applied flux (no points). Only the two channels with applied signal show substantial response, except for a ≈2% crosstalk to the subsequent channels.

3. MILESTONES IN SUPERCONDUCTING BOLOMETER ARRAY DEVELOPMENT

3.1 Fundamental component verification

We have demonstrated many aspects of the technologies for making useful arrays of superconducting bolometers. The most important first step is to produce a TES bolometer with the expected noise performance. This is shown in Figure 8.

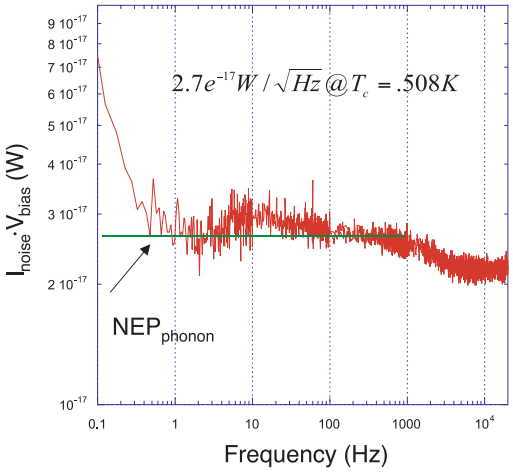

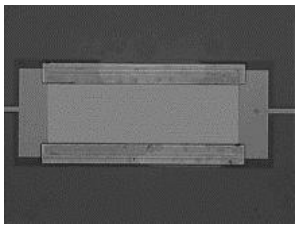

Figure 8. (L) Noise readout of a Mo/Cu bilayer TES, showing performance close to the theoretically predicted phonon noise. (R) Photo of the device.

Since large arrays of superconducting bolometers require SQUID multiplexers, it is necessary to demonstrate that this readout can perform adequately. Figure 7 above (from Benford et al. 2000[9]) shows that the crosstalk between channels is low enough to be small compared to typical optical crosstalk present in imaging arrays. Figure 9 below is a noise spectrum of the Johnson noise of a set of resistors, read out in multiplexed mode, from Staguhn et al. (2001)[16]. It proves that the SQUIDs can read out many channels without introducing excess noise, an important point for scalability to large (~100 element) SQUID multiplexers.

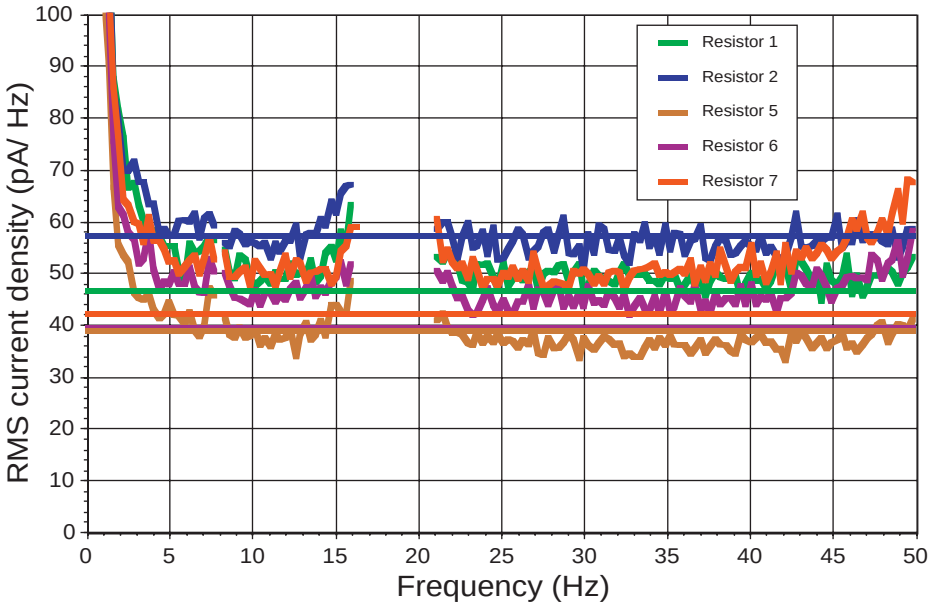

Figure 9. Spectrum of the Johnson noise of a set of resistors, simultaneously read out by a multiplexed SQUID amplifier. This data has had noise features from wiring resonances at 7Hz and 18Hz removed. The expected Johnson noise is shown as horizontal lines, and matches the observed noise closely. There is little excess noise produced by using a multiplexed SQUID readout.

3.2 Optical Use of Multiplexed Bolometers

To demonstrate that a multiplexed superconducting bolometer works as a system, it is necessary to show that it can actually be used to detect light. Benford et al. (2000)[9] conducted tests to verify this performance, and have shown that the detectors operate as expected. Additionally, these tests were used to verify the photometric performance of TES bolometers, showing good linearity and 80±10% optical efficiency with a tuned cavity. Furthermore, an upper limit of the response time of 2ms was shown.

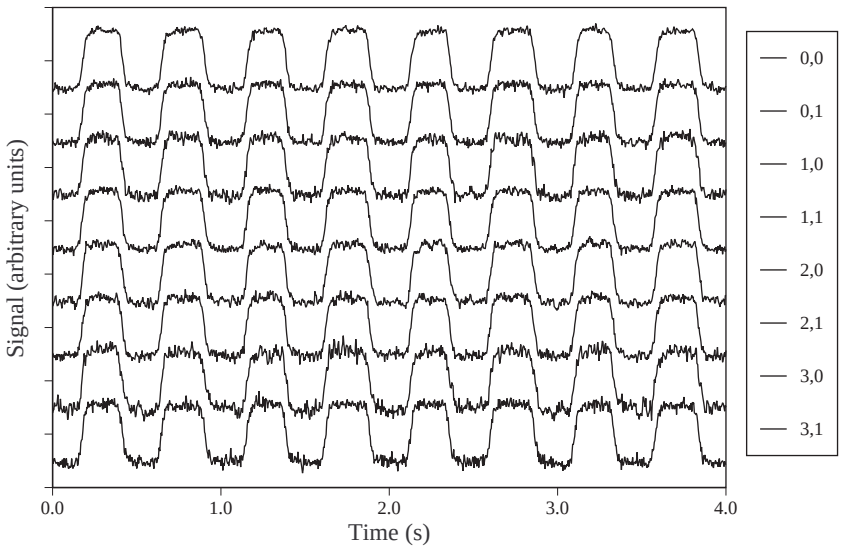

Figure 10. Multiplexed detection of light from 8 detectors read out simultaneously while observing a chopped hot/cold blackbody. These data, and other data on the same devices, demonstrated that a highly efficient, fast, linear TES bolometer array could be read out with SQUID multiplexed amplifiers.

3.3 Astronomical Use of Multiplexed Superconducting Bolometers

An instrument using multiplexed superconducting bolometers was delivered to the Caltech Submillimeter Observatory on Mauna Kea, in part to validate this technology in an astronomical setting. The results of this observing run are presented elsewhere[17,18]. Due to extremely poor weather, the only data taken were skydips to measure the atmospheric opacity and a chopped observation across the Moon limb (Figure 11). Both results showed that the detectors were operational.

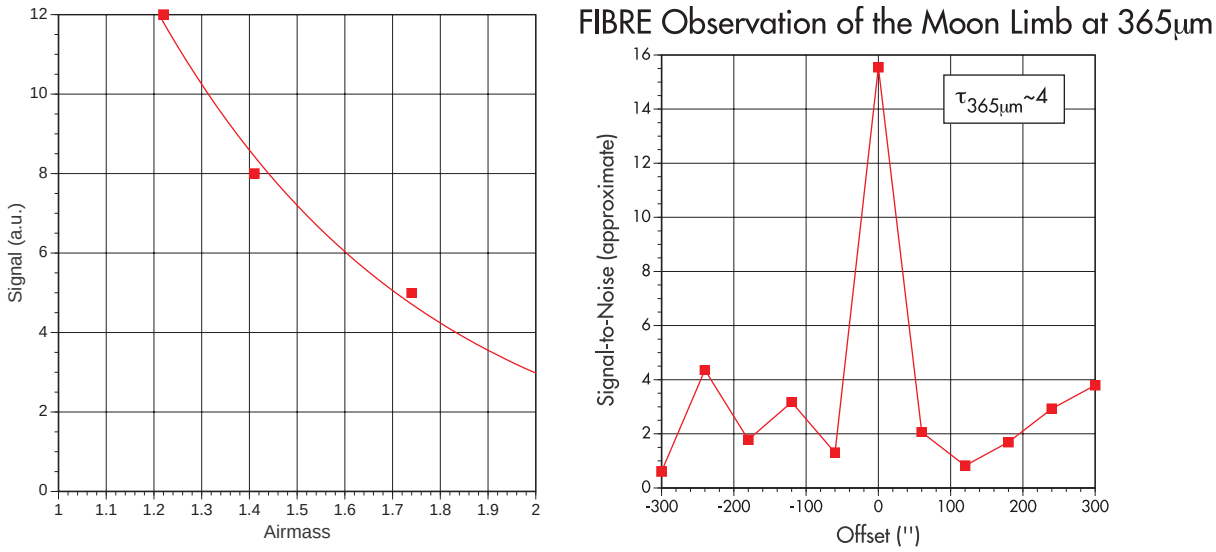

Figure 11. First astronomical use of multiplexed superconducting bolometer arrays. A Fabry-Perot spectrometer named FIBRE was used to detect emission in the 350μm band using the Caltech Submillimeter Observatory. (L) Skydip showing the response to atmospheric emission, when the in-band opacity was τ~3. (R) Response of a detector scanned across the Moon limb while chopping; the edge is clearly visible.

4. SCALING SMALL DETECTOR ARRAYS INTO LARGE DETECTOR ARRAYS

4.1. Arraying Strategies

The largest cryogenic bolometer arrays current available are manufactured by NASA's Goddard Space Flight Center using the "Pop-Up Detector" (PUD) architecture. In this approach, a linear array of bolometers using thin silicon beams to support large absorbers is designed so that it can be folded, causing the absorbers to "pop up" above the folded frame. When several of these linear arrays are stacked side-by-side to form a close-packed, two-dimensional array, the wiring is brought out behind the focal plane. The current state-of-the-art is the HAWC and SHARC-II arrays, each containing 384 (12x32) detectors (Figures 12 and 13). A PUD architecture array using superconducting transition edge sensor (TES) bolometers is being built for the SAFIRE instrument on SOFIA[19] that will feature a 512 detectors (16x32), and can be extended to 1k detectors (32^2)[20]. It is reasonable to assume that when larger SQUID multiplexers become available (with 128 inputs being within reason with present technology), array formats of up to 128^2 might be plausible.

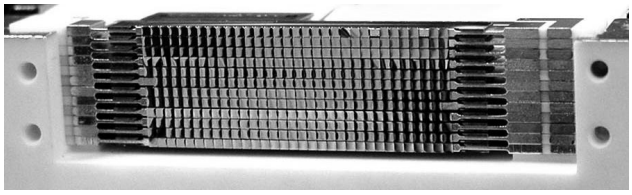

Figure 12. 12x32 PUD bolometer array manufactured for SHARC II and HAWC, currently the largest cryogenic bolometer array yet manufactured.

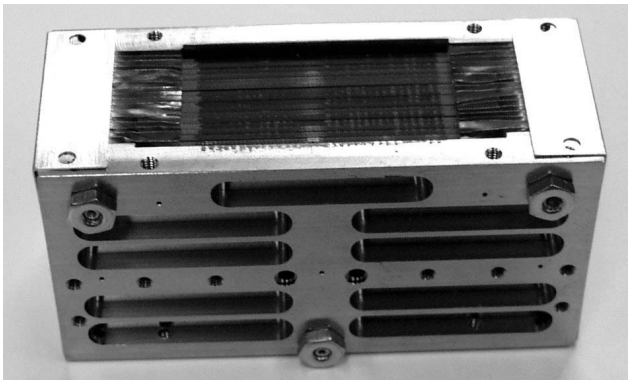

Figure 13. Mechanical prototype 16x32 superconducting bolometer array for SPIFI and SAFIRE; this package houses both bolometers and SQUID multiplexers.

As bolometer array formats continue to increase, changing from a stacked PUD array design to a monolithically planar array seems inevitable. One example of this is the planar feedhorn-coupled array, which has had great success with the BOOMERANG and BOLOCAM "spiderweb" arrays[21], but is known to be a factor of ~3.6 slower in mapping speed than an equivalent filled array[22]. An example of GSFC-manufactured mechanical model arrays for feedhorn-coupling is shown in Figure 14. The web-like structure satisfies one of the requirements in the development of monolithic close-packed planar arrays, the production of thermally isolated bolometer suspension. It may also be possible to produce planar structures with more compact thermal isolation, shown schematically in Figure 15. Such arrays could be absorber-coupled, providing an optical fill fraction of ~90%.

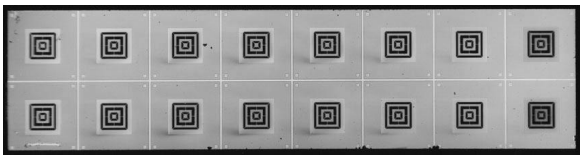

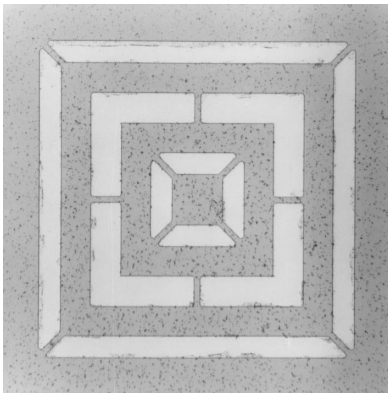

photos courtesy Tina Chen, Barbara Campano, Alex Bier, Elmer Sharp

Figure 14. (Above) a 2x8 mechanical prototype for feedhorn-coupled arrays. The pixel pitch is 2mm. (Left) enlargement of the thermally isolating structure. Only the central square is designed to absorb light; the remainder of the structure is supposed to prevent ballistic phonon propagation.

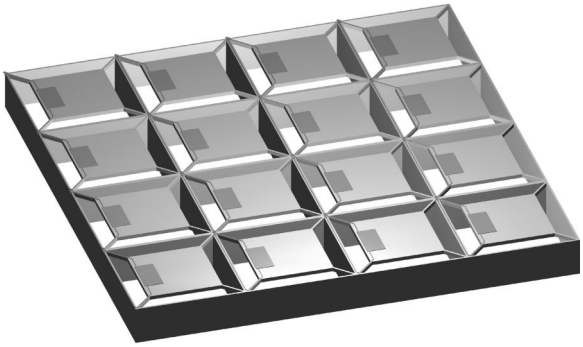

Figure 15. Illustration of a compact geometry for absorber-coupled planar superconducting bolometer arrays.

We have manufactured mechanical prototypes of planar close-packed, absorber-coupled bolometers. In these initial attempts, we chose to produce 3x3 arrays with 3mm absorbers, suitable for use at millimeter wavelengths from ground-based telescopes. This small array size permits several different mechanical designs to be fabricated on a single silicon wafer. The most robust leg geometry we have found is shown in Figure 16.

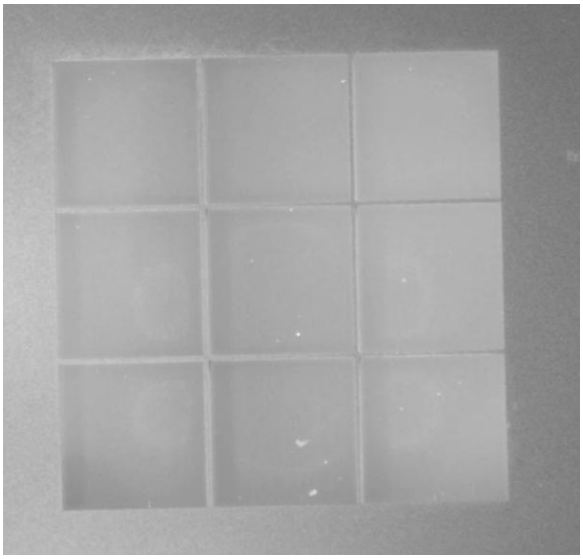

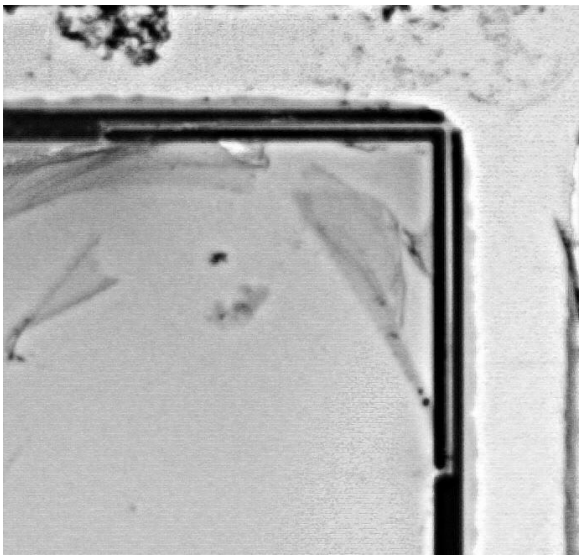

Figure 16. (Left) Sample 3x3 array of bolometers isolated by short legs from a grid of thin beams (in this picture, the membrane has yet to be etched). (Right) Enlargement of the corner of one bolometer, showing the thin thermally isolating legs; some residual metallization from processing remains.

4.2. Mechanical Assembly:

Someday, space flight missions like SAFIR, CMBPOL, and SPECS will need large detector arrays. Ultimately, simple construction, compact design, and the capability of processing bolometers with as little skilled craftsmanship as possible are all desirable. Planar arrays such as the sketch at right (Figure 17) are a goal. In this implementation, a single wafer of detectors and a single wafer of readouts are bump-bonded together to form a hybrid integrated detector array. The arrays shown in Figure 16 are being designed with this purpose in mind. For the time being, a circuit board can fan out the wiring to the SQUID amplifiers. One technology to be demonstrated before the hybridized array at right is possible is the development of superconducting bump bonds.

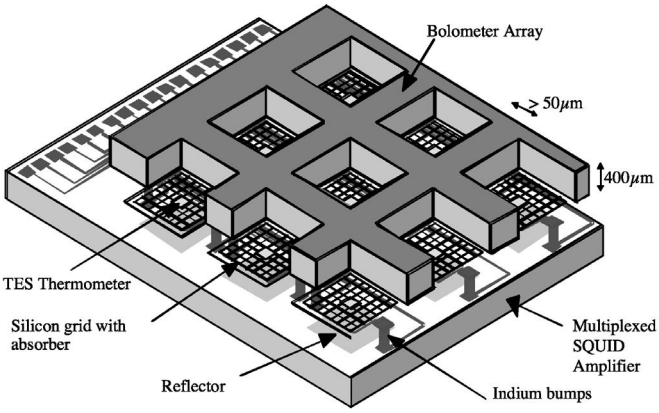

Figure 17. Hybrid planar array with multiplexers.

5. DETECTORS FOR SPACE APPLICATIONS

5.1. Sensitivity Requirements

The most demanding detector arrays in the future of space applications are those required for the SAFIR mission, as outlined in Benford et al. (2002)[8]. One of the challenges is that for a camera or low-resolution spectrometer, the NEP required is $<10^{-19}$ W/√Hz. This is about 100 times better than detectors being developed for ground-based and airborne bolometers[18,20]. In addition, the array format needs to be larger, requiring perhaps 16 kilopixels as opposed to the 1/2 kilopixel arrays being developed today.

The NEP of a phonon-noise-limited superconducting bolometer can be calculated easily ($NEP_{phonon} = \sqrt{2kT_C^2 \overline{G}}$, given a thermal conductance $G(T)$). For a superconducting TES, the detector will saturate when the combined optical (P_{opt}) and electrical bias (P_{elect}) power exceed the power thermally conducted away by the bolometer supports:

$$P_{opt} + P_{elect} \geq \int_{T_{\rm sink}}^{T_c} G(T)dT\,,$$

where T_c and $T_{\rm sink}$ are the transition temperature and the thermal sink temperature, respectively. The GSFC bolometer design[9] using micromachined silicon nitride structures could yield a thermal conductance of $G(T) \approx 5 \cdot 10^{-11}\ T^3$ W/K. Such a detector could be used for a broadband instrument, since the phonon-limited NEP of such a bolometer is $1 \cdot 10^{-19}$ W/√Hz at a transition temperature of around 0.1K. When biased suitably, the maximum saturation power is obtained with negligible electrical power and a sufficiently low sink that its temperature is unimportant: $P_{sat} = 1.25 \cdot 10^{-11}\ T_c^4$ W. In this case, the saturation power will be ~5fW, equivalent to flux densities of order 10mJy. Such a camera will be blinded by all sources detected by IRAS. A similar detector array with a T_C of ~0.065K would be able to achieve the sensitivity necessary for a low resolution spectrometer of resolving power $\lambda/\Delta\lambda \sim 100$. Going to a spectrometer with a resolving power of $\lambda/\Delta\lambda \sim 2000$ would require a sink temperature of about 0.015K to yield a low enough phonon noise.

5.2. Dynamic Range

When designing an instrument to take advantage of the ultimate sensitivity of the TES – typically featuring low transition temperature and low thermal conductance – the risk of saturating detectors at a moment where you want to take data is unacceptable. Conditions under which saturation occur when high power is deposited in the detector, as in prolonged periods of high backgrounds or scans that pass briefly over point sources that are bright in the signal band. A device with a higher transition temperature, and the associated higher thermal conductance, would be able to absorb more power before saturation. A single bolometer with two TES sensors could take advantage of the high saturation power of the upper transition and still be photon noise limited while also having an "ultrasensitive" mode when it is

possible to bias on the lower transition. One disadvantage is that such a bolometer would ordinarily require two readout circuits.

To begin with, we consider a generic TES bolometer with a thermal conductance $G(T)=G_1T^{\xi}$ derived from mechanical isolation or electron-phonon decoupling. The saturation power for this bolometer is:

$$P_{saturation} \equiv \int_{T_{bath}}^{T_{C1}} G(T)\, dT \approx \frac{G_1\, T_{C1}^{\xi+1}}{\xi+1} \tag{1}$$

assuming that the bath temperature T_{bath} is small compared to the transition temperature T_{C1}. The phonon noise equivalent power is also related to this thermal conductance:

$$NEP_{phonon} = \sqrt{2kT^2\overline{G}} \approx \sqrt{2kT_{C1}^{\xi+2}\frac{G_1}{\xi+1}}. \tag{2}$$

If we define the dynamic range $\Re$ to be the ratio of the saturation power to the NEP, this figure of merit becomes:

$$\Re \equiv \frac{P_{saturation}}{NEP_{phonon}} = \sqrt{\frac{G_1}{2k(\xi+1)}\cdot T_{C1}^{\xi}} \text{ and therefore } \Re = \sqrt{\frac{P_{saturation}}{2kT_{C1}}} = \frac{NEP_{phonon}}{2kT_{C1}}.$$

For a bolometer optimized for a given background-limited noise performance or for a given maximum background power, lowering the transition temperature will improve the dynamic range. However, the design requirement of the low background of a cryogenic space telescope will push the noise performance while still requiring high saturation powers. Consistent with this goal, equations (1) and (2) show that the dynamic range can be improved by increasing the geometric factor G_1 and lowering T_{C1} to compensate. At some point, practical considerations will prevent the increasing of G_1 or the lowering of T_{C1}. At this point, one possibility is to produce a device with multiple transition temperatures. In the simplest implementation, two TES devices would be placed in series, both isolated by the same thermal conductance. If the second device has a transition temperature $T_{C2}>T_{C1}$, the dynamic range becomes:

$$\Re_{two-T_C} = \frac{\int^{T_{C2}} G(T)\, dT}{NEP_{phonon}} = \sqrt{\frac{G_1}{2k(\xi+1)}\cdot\frac{T_{C2}^{2\xi+2}}{T_{C1}^{\xi+2}}} = \left(\frac{T_{C2}}{T_{C1}}\right)^{\xi+1}\cdot\Re.$$

If the transition temperature ratio is 2 and the thermal isolation is provided by a dielectric material of $\xi\approx 3$, the two-T_C detector provides an increase in dynamic range of an order of magnitude. A two-T_C device with a temperature ratio of 10 could provide 10^4 improvement in dynamic range. The disadvantage of this approach is that it reduces the phonon noise margin over photon noise by a factor of $(T_{C2}/T_{C1})^{1/2}$. However, such devices are not difficult to fabricate and might be easily implemented with a small heater on every bolometer. The idea of direct pixel heating has thee advantage that the entire array can easily be switched between the high sensitivity mode and the high saturation mode. Furthermore, the heater can be used to improve the DC stability, perhaps resulting in more stable and linear detector arrays.

We have fabricated detectors that feature two TES detectors in series, biased such that one TES is on its transition, while the other is either superconducting or normal. The resistance of a Mo/Cu two-T_C TES is shown in Figure 18. This device is fabricated by a process in which a liftoff Cu feature makes edge bars on one detector and a lower T_C device on the second detector. The sensitivity of the transitions is about α=200 for the higher T_C and α=100 for the lower T_C. When placed on an isolated bolometer membrane (which has not yet been done), the ratio in saturation powers would differ by a factor of ~4, while the noise changes by a ratio of ~2.4 (for example, between $4\cdot10^{-18}$ W/√Hz and 10^{-17} W/√Hz). We have also manufactured single structures where the regions of the two transitions are in immediate proximity. We are exploring different designs for accomplishing the desired resistance ratio for two-T_C performance as well as to examine interactions under bias conditions.

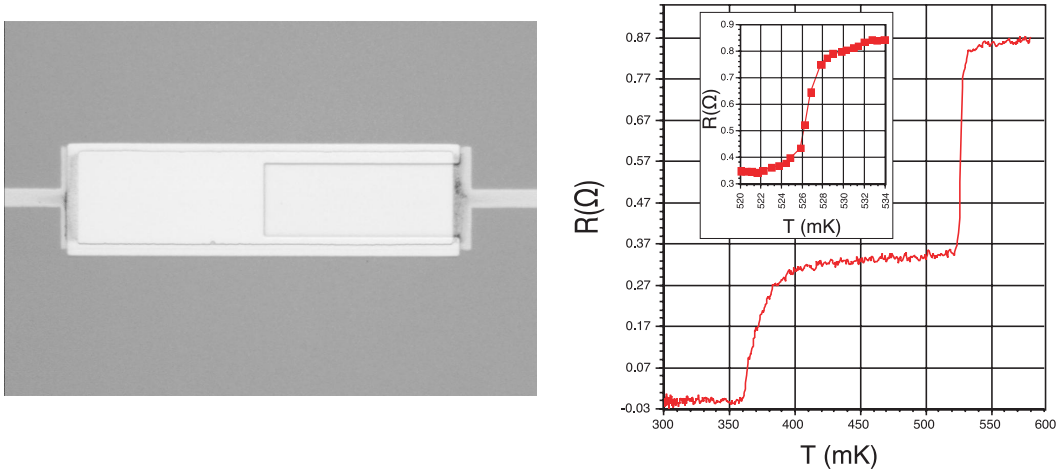

Figure 18. Two-transition Mo/Cu TES. The thicker copper layer at left is used as the normal metal bar to control edge effects on the higher-T_C device. The two transitions at 365mK and 527mK are evident.

Our first demonstration two-T_C detector used a shadow-masked Al/Ag TES bilayer with transition temperatures of 265mK and 510mK. The noise is shown at right in Figure 19. Based on this noise measurement, the predicted powers (assuming an index in the thermal conductivity of ~2) are 2pW and 14pW. The voltage-current relation for this device is shown in Figure 20, along with the inferred resistance (calculated from the measured Johnson noise). An excellent agreement between the calculated power and measured power on the transitions is seen. Although the sharpness of these transitions is hardly superior, the measurement method may have inaccuracies. It is clear that the IV curve shows two distinct regions of electrothermal feedback (separated by a large region where the device is current biased on the upper part of the transition.). This indicates that the detectors are operating with feedback, and so the transition must be fairly sharp. The noise measurements were made when the detector was biased onto the steep parts of each superconducting transition.

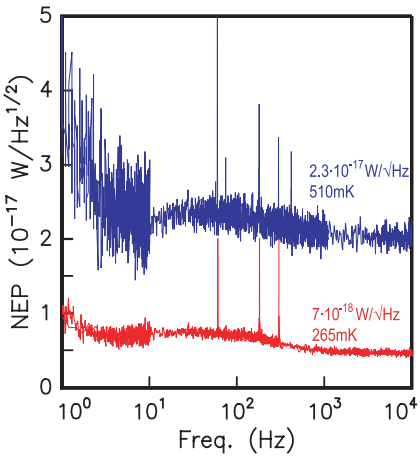

Figure 19. Noise of a two-T_C bolometer when biased onto each transition.

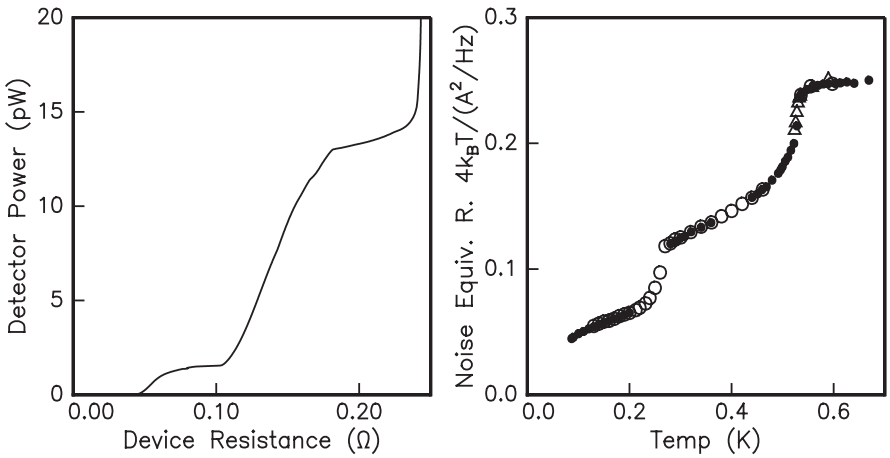

Figure 20. (L) Power vs. resistance in a dual-T_c TES (R) Resistance vs. temperature of the same device

5.3. Temperature Limit

There is a fundamental limit present in superconducting bolometer arrays, due to the fact that the detector phonon noise can be derived from the optical photon noise. In the simplest terms, the phonon noise: $NEP_{phonon}=(4kT^2G)^{1/2}$, where G is the thermal conductance at temperature T. The maximum power seen before saturation is then $P_{sat}\approx GT_C/\eta$, where $\eta\sim10$ is a factor derived from the thermal conductivity index and the ratio between T_C and the base temperature. The photon noise in the nearly-saturated case is $NEP_{photon}=(2Ph\nu)^{1/2}$. Rearranging, we find that $2kT_C\eta \ll h\nu$ in order to keep phonon noise below photon noise. As an example, the temperature for operation with 10% excess noise at $\lambda\sim1$mm is ~300mK.

5.4. Optical Coupling

There have been two common approaches in coupling far-infrared and submillimeter radiation into direct detectors. For bolometers, the most common approach has been to use feedhorns or other concentrators to capture light from an area at least λ in size and focus it down to a smaller detector. This has the advantage that the efficiency of such a horn optimally coupled to a telescope and pointed directly at a source is the best realizable. However, it is not possible to optimize the feedhorn and simultaneously produce Nyquist sampling of the image plane of the telescope. As an alternative to this approach, we have built the filled arrays of absorbers as shown in Figure 12. Such an array is not as efficient per pixel, but as it accepts all spatial information simultaneously, the mapping speed of the array is roughly three times better than it is for the feedhorn-coupled arrays[22]. The price one pays for this efficiency is that more pixels are required, and there must be a cold optics box surrounding the detectors that completely defines the beam. These two options are shown in Figure 21. The left panel shows a 32x32 feedhorn array for 400GHz operation that we are developing for use with large format planar bolometer arrays. The technology required to produce one such feedhorn – typically by electroforming – is not easily scaled to such large arrays. Our approach uses plates with grids of appropriate holes, which build up to form an arbitrarily large array of feedhorns.

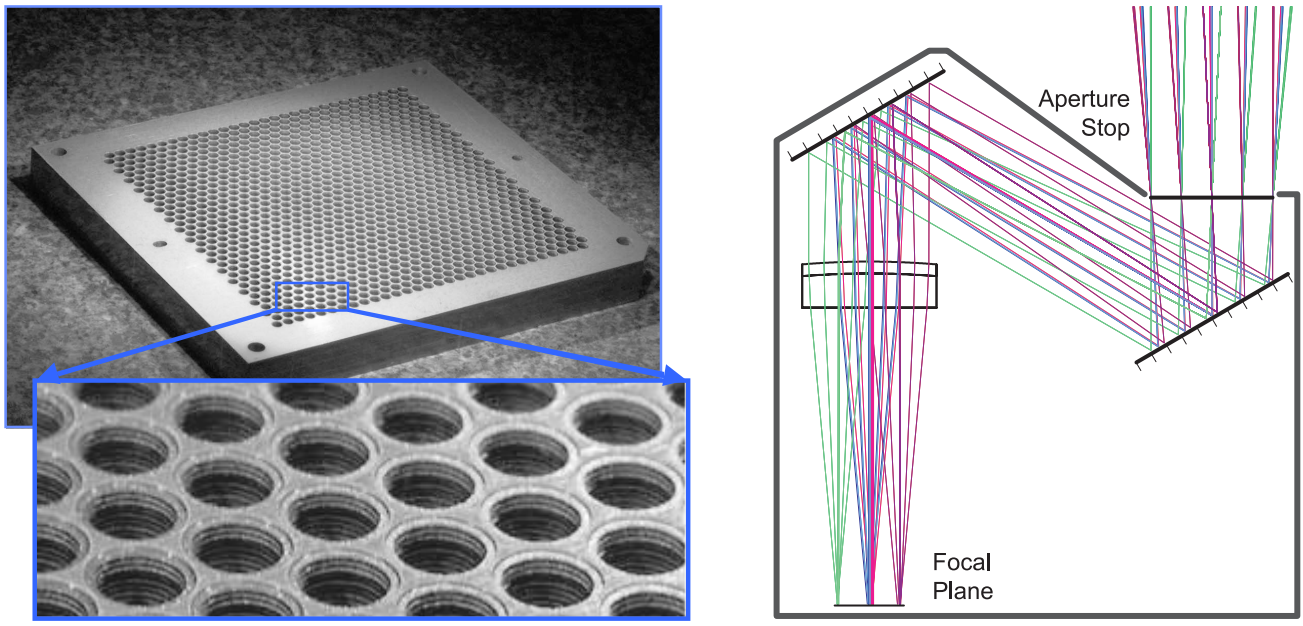

Figure 21. (L) 32x32 array of 400GHz feedhorns for close-packed, single-moded beam definition (R) Optical approach to beam definition, which can be used with filled arrays to provide the desired coupling to modes on the sky.

6. SUMMARY

Superconducting transition edge sensor bolometers have many good features for use as sensitive detectors for far-infrared and submillimeter wavelengths. TES detectors feature good noise performance, high sensitivity, high speed, linear behavior, and few strange effects. All the components of TES multiplexed arrays have been demonstrated. Low-noise operation, nearly noiseless multiplexed readouts, and systems issues associated with astronomical instruments have all been shown. As a practical issue, superconducting bolometers and their associated superconducting amplifiers have

much simpler thermal interfaces than semiconducting bolometers. Furthermore, SQUID multiplexed readouts have been developed, permitting large arrays with simple, scalable electronics. Investigations of the details of noise mechanisms in TES detectors are ongoing, as are efforts to improve the dynamic range through the use of dual-transition bolometers. Fabrication issues are well understood, and transition edge sensor bilayers for large arrays can be made using thin film micromachining techniques and robust superconducting materials systems. We are also developing close-packed architectures to permit large format (>1000 elements) filled arrays with high efficiency. Future space missions require a substantial advance in far-infrared detector technology, with substantially more pixels of higher sensitivity than have been made to date. TES bolometer arrays are the most promising technology for meeting the sensitivity and pixel count requirements of upcoming missions in the far-infrared to millimeter wavelength range such as SAFIR and CMBPOL.

REFERENCES

1. *"Astronomy and Astrophysics in the New Millennium"*, National Academy Press, Washington, DC 2001
2. Harvey, P.M., Rieke, G.H., Lester, D.F., & Benford, D.J. 2002, Proc. SPIE #4850, in press; *"Single Aperture Far-Infrared Observatory (SAFIR)"*
3. Amato, M.J., Benford, D.J., Moseley, S.H., & Roman, J. 2002, Proc. SPIE #4850, in press; *"An Engineering Concept and Enabling Technologies for a Large Single Aperture Far-Infrared Observatory (SAFIR/)"*
4. Mather, J.C. et al. astro-ph/9812454, *"The Submillimeter Frontier: A Space Science Imperative"*
5. Voellmer, G.M. et al. 2002, these proceedings; *"Design and Fabrication of Two-Dimensional Semiconducting Bolometer Arrays for HAWC and SHARC-II"*
6. *"The Decade of Discovery in Astronomy and Astrophysics"*, National Academy Press, Washington, DC 1991
7. Richards, P.L. 2002, Proceedings of "Far-IR, Sub-MM & MM Detector Technology Workshop", in press; *"Bolometric Detectors for Space Astrophysics"*
8. Benford, D.J., Chervenak, J.A., Irwin, K.D., & Moseley, S.H., Proc. SPIE #4850, in press; *"Ultralow-Background Large-Format Bolometer Arrays"*
9. Benford, D.J. et al. 2000, IJIMW 21 (12), pp.1909-1916; *"Multiplexed Readout of Superconducting Bolometers"*
10. Figueroa, E. private communication
11. Lindeman, M.A.& De Korte, P.A.J., private communications
12. Cabrera, B., Clarke, R.M., Colling, P., Miller, A.J., Nam, S. & Romani, R.W. 1998, APL, 73, pp.735-737; *"Detection of Single Infrared, Optical, and Ultraviolet Photons Using Superconducting Transition Edge Sensors"*
13. De Korte, P.A.J., private communication
14. Chervenak, J.A., Irwin, K.D., Grossman, E.N., Martinis, J.M., Reintsema, C.D. & Huber, M.E. 1999, Applied Physics Letters, 74, pp. 4043-4045; *"Superconducting Multiplexer for Arrays of Transition Edge Sensors"*
15. Irwin, K.D., Hilton, G.C., Wollman, D.A., & Martinis, J.M., 1998, Journ. Appl. Phys. 83, p. 3978; *"Thermal-Response Time of Superconducting Transition Edge Sensors"*
16. Staguhn, J.G. et al. 2001, AIP Conference proceedings #605, "Low Temperature Detectors", ed. by F.S. Porter et al., pp.321-324; *"TES Detector Noise Limited Readout Using SQUID Multiplexers"*
17. Benford, D.J. et al. 2001, AIP Proc. #605, "Low Temperature Detectors", ed. by F.S. Porter et al., pp.589-592; *"First Astronomical Use of Multiplexed Transition Edge Bolometers"*
18. Staguhn, J.G. et al. 2002, these proceedings; *"Astronomical Demonstration of Superconducting Bolometer Arrays"*
19. Benford, D.J., Moseley, S.H., Stacey, G.J., Shafer, R.A. & Staguhn, J.G. 2002, Proc. SPIE #4857, in press; *"Far-infrared imaging spectroscopy with SAFIRE on SOFIA"*
20. Benford, D.J., Voellmer, G.M., Chervenak, J.A., Irwin, K.D., Moseley, S.H., Shafer, R.A. & Staguhn, J.G. 2002, Proc. SPIE #4857, in press; *"Design and Fabrication of a Two-Dimensional Superconducting Bolometer Array for SAFIRE"*
21. Mauskopf, P.D. et al. 2000, in "Imaging at Radio through Submillimeter Wavelengths", ASP #217, p.115; *"BOLOCAM: a 144 Element Bolometer Array Camera for Millimeter-Wave Imaging"*; Crill, B.P. et al. 2002, ApJ, submitted; *"BOOMERANG: A Balloon-borne Millimeter Wave Telescope and Total Power Receiver for Mapping Anisotropy in the Cosmic Microwave Background"*
22. Griffin, M.J., Bock, J.J., & Gear, W.K. 2002, Applied Optics, submitted; *"The Relative Performance of Filled and Feedhorn-Coupled Focal-plane Architectures"*